Published in final edited form as:

Hepatology. 2015 October ; 62(4): 1227–1236. doi:10.1002/hep.27956.

NHERF-1 knockout mice have an attenuated hepatic inflammatory response and are protected from cholestatic liver injury

Man Li[1], **Albert Mennone**[1], **Carol J. Soroka**[1], **Lee R. Hagey**[2], **Xinshou Ouyang**[1], **Edward J. Weinman**[3,4], and **James L. Boyer**[1]

Man Li: man.li@yale.edu; Albert Mennone: al.mennone@yale.edu; Carol J. Soroka: carol.soroka@yale.edu; Lee R. Hagey: lhagey@ucsd.edu; Xinshou Ouyang: xinshou.ouyang@yale.edu; Edward J. Weinman: eweinman1440@yahoo.com; James L. Boyer: james.boyer@yale.edu

[1]Yale Liver Center, Yale University School of Medicine, New Haven, CT

[2]Department of Medicine, University of California, San Diego, La Jolla, CA

[3]Department of Medicine, Baltimore, MD

[4]Department of Physiology, University of Maryland School of Medicine, Baltimore, MD

Abstract

The intercellular adhesion molecule-1 (ICAM-1) is induced in mouse liver after bile duct ligation (BDL) and plays a key role in neutrophil-mediated liver injury in BDL mice. ICAM-1 has been shown to interact with the cytoskeletal ezrin-radixin-moesin (ERM) proteins that also interact with the PDZ protein, Na+/H+ exchanger regulatory factor 1 (NHERF-1/EBP50). In NHERF-1$^{-/-}$ mice, ERM proteins are significantly reduced in brush border membranes from kidney and small intestine. ERM knockdown reduces ICAM-1 expression in response to TNF-α. Here we show that NHERF-1 assembles ERM proteins, ICAM-1 and F-actin into a macromolecule complex that is increased in mouse liver after BDL. Compared with wild-type (WT) mice, both sham-operated and BDL NHERF-1$^{-/-}$ mice have lower levels of activated ERM and ICAM-1 protein in the liver accompanied by significantly reduced hepatic neutrophil accumulation, serum ALT, and attenuated liver injury after BDL. However, total bile acid concentrations in the serum and liver of sham and BDL NHERF-1$^{-/-}$ mice were not significantly different from the WT controls, although hepatic tetrahydroxylated bile acids and Cyp3a11 mRNA levels were higher in NHERF-1$^{-/-}$ BDL mice.

Conclusion—NHERF-1 participates in the inflammatory response that is associated with BDL induced liver injury. Deletion of NHERF-1 in mice leads to disruption of the formation of ICAM-1-ERM-NHERF-1 complex and reduction of hepatic ERM proteins and ICAM-1, molecules that are up-regulated and are essential for neutrophil-mediated liver injury in cholestasis. Further study of the role of NHERF-1 in the inflammatory response in cholestasis and other forms of liver injury should lead to discovery of new therapeutic targets in hepatic inflammatory diseases.

Corresponding author: James L. Boyer, MD, Department of Medicine, Yale University School of Medicine, 333 Cedar Street/1080 LMP, P.O. Box 208019, New Haven, CT 06520-8019, USA; Tel.: 203-785-5279; Fax: 203-785-7273; james.boyer@yale.edu.

Keywords

PDZ proteins; ERM proteins; intercellular adhesion molecule-1; cholestasis; inflammation

INTRODUCTION

Cholestasis is characterized by rapid elevation of bile acid levels in the liver and plasma, followed by hepatocyte injury and bile duct proliferation, and, if progressive, liver fibrosis and cirrhosis (1, 2). While various causes of cholestasis have been well described, the molecular mechanisms of cholestatic liver injury remain largely undefined. One major hypothesis notes that the accumulation of highly toxic hydrophobic bile acids within hepatocytes is the direct cause of hepatocellular death (3–5). This hypothesis is based mainly on work in cultured rat hepatocytes treated with high concentrations (50 μM or 100μM) of pro-apoptotic bile acids, such as glycochenodeoxycholic acid (GCDCA) and taurolithocholic acid (TLCA) (6–9), as well as in mice fed lithocholic acid (LCA) (10). However, studies using bile duct ligation (BDL), a well-established cholestasis model, suggest that cholestatic liver injury may be caused largely by the inflammatory response involving neutrophil-mediated liver cell necrosis (11, 12). This view is supported by the infiltration of neutrophils around the site of injury in mouse liver within eight hours after BDL and their predominance during this acute phase of liver injury (12, 13). In addition, the bile acid species that increase the most in concentration in the serum after BDL in mice are relatively non-toxic hydrophilic bile acids such as TCA, β-muricholic acid (βMCA) and tauro-β-muricholic acid (TβMCA). Exposure of cultured mouse hepatocytes to even millimolar concentrations of a mixture of these bile acids does not cause apoptosis or necrosis, but substantially induces expression of pro-inflammatory genes such as intercellular adhesion molecule-1 (ICAM-1) (14).

ICAM-1 is an immunoglobulin-like cell adhesion molecule that is expressed at low levels in endothelial cells under normal conditions. After BDL, ICAM-1 is upregulated in both hepatic endothelial and parenchymal cells (15). ICAM-1 mediates neutrophil-endothelial as well as neutrophil-hepatocellular interactions by binding to β_2-integrins that are expressed on the neutrophil cell surface (16, 17) (Fig. 1). Liver necrosis is dramatically reduced in ICAM-1 deficient mice after BDL, and is accompanied by a decrease in hepatic infiltration of neutrophils, suggesting that liver injury induced by BDL is neutrophil-dependent (15).

Recently ERM proteins, ezrin, radixin and moesin, have been discovered to also influence leukocyte migration across the endothelial barrier to the site of inflammation. ERM proteins are a family of homologous proteins that interact with numerous partners including membrane proteins, phospholipids, actin cytoskeleton and signaling molecules, and organize multiprotein complexes that subserve diverse functions including cell morphogenesis, endocytosis/exocytosis, adhesion and migration (18–20) in specific cellular compartments. In TNF-α-stimulated human umbilical vein endothelial cells (HUVEC), activated ERM proteins have been shown to interact with ICAM-1 and vascular cell adhesion molecule-1 (VCAM-1) (21). Together with filamentous actin, these proteins form microvilli-like membrane projections called docking structures that anchor and partially embrace the

leukocyte to promote firm leukocyte adhesion and initiate leukocyte transendothelial migration (21, 22) (Fig. 1). ERM proteins play a role in ICAM-1 protein expression and increases in cellular permeability in response to inflammation. ERM knockdown inhibits ICAM-1 upregulation in HUVEC as well as cytoskeletal rearrangement and permeability increases induced by TNF-α in pulmonary microvascular endothelial cells (23, 24).

ERM proteins exist in a dormant conformation in the cytoplasm and become activated upon binding to phosphatidylinositol 4, 5-bisphosphate (PIP2) and phosphorylation by kinases. Phosphorylated ERM can bind to membrane proteins directly or indirectly by binding to the Na+/H+ exchange regulatory factor-1 (NHERF-1). NHERF-1, also known as ERM-binding phosphoprotein 50 (EBP50), is abundantly expressed beneath apical membranes of polarized epithelial cells such as hepatocytes and bile duct epithelial cells (25). It's a scaffolding protein that interacts with membrane proteins through its two PDZ domains, and therefore assembles and coordinates functionally-related signaling proteins into integrated macromolecule complexes (26). NHERF-1 interacts with ERM proteins via its ERM-binding motif and regulates the expression of ERM proteins at the apical membrane of polarized cells. In NHERF-1$^{-/-}$ mice, ERM proteins are significantly reduced in brush border membranes from kidney and small intestine (27). However, the roles of NHERF-1 and ERM proteins in neutrophil-mediated liver injury in cholestasis remain unclear. We hypothesized that NHERF-1 assembles ERM proteins, ICAM-1 and F-actin into a macromolecule complex that plays a role in neutrophil infiltration in mouse liver and that deficiencies in NHERF-1 disrupt the formation of this complex and affect expression of hepatic ERM proteins and ICAM-1, thereby influencing neutrophil accumulation and cholestatic liver injury induced by bile duct ligation.

MATERIALS AND METHODS

Animals and Cells

See the Supplemental Materials. NHERF-1$^{-/-}$ mice were generated as previously described (28). Wild-type (WT) C57BL/6 mice were purchased from the Jackson Laboratory (Bar Harbor, Maine). Age matched (13–17 weeks) male mice were used for the present studies. Animals were housed in a temperature- and humidity-controlled room under a light cycle with free access to food and water. BDL was performed under sterile conditions as previously described from this laboratory (29). Control animals underwent sham surgery in which the bile duct was exposed, but not ligated. Tissues and serum were collected 7 days after surgery. Mice were fasted overnight and all animals were sacrificed between 8 AM and 11 AM. Tissues were flushed with normal saline, snap frozen in liquid nitrogen and stored at −80°C until used. All experimental protocols were approved by the local Animal Care and Use Committee, according to criteria outlined in the "Guide for the Care and Use of Laboratory Animals" prepared by the National Academy of Sciences, as published by the National Institutes of Health (NIH publication 86-23, revised 1985).

Co-Immunoprecipitation (Co-IP)

Co-IP was performed using a Thermo Scientific Pierce Co-Immunoprecipitation Kit (Pierce Biotechnology, Rockford, IL) according to the manufacturer's instructions. Briefly, mouse

liver tissue was homogenized in IP Lysis/Wash Buffer (25mM Tris, 150mM NaCl, 1mM EDTA, 1% NP-40, 5% glycerol, pH 7.4, supplemented with protease and phosphatase inhibitor cocktails (Pierce)) and the tissue debris was removed by centrifugation at 13000×g for 10 min. Four milligrams of liver protein was pre-cleared with control agarose resin and incubated overnight at 4°C with agarose resin coupled with a rat anti-mouse ICAM-1 antibody (Pierce). A Co-IP reaction using inactivated agarose resin from the Co-IP kit incubated with liver lysates served as a negative control for the experiment. After washing 4 times with the IP Lysis/Wash Buffer the resin was eluted with the Elution Buffer (pH2.8) and the eluate analyzed by immunoblotting.

Liver Histology and Neutrophil Staining

Formalin-fixed liver tissue was paraffin-embedded and sections were stained with hematoxylin and eosin. Necrosis was assessed by blinded morphometric analysis. Immunohistochemistry was performed using a rat monoclonal antibody to Ly-6B.2 alloantigen (AbD Serotec) and a peroxidase/DAB substrate kit (Vector Lab, Burlingame, CA). Neutrophil accumulation was quantitated with ImageJ.

Bile Acid Measurements and Liver Function Tests

Liver tissue was extracted in 75% ethanol (100 mg/ml) for bile acid measurement. Total bile acid concentration in serum and extracted liver was measured using an assay kit (Diazyme Laboratories, Poway, CA). Serum levels of alanine aminotransferase (ALT) and alkaline phosphatase (ALP) were measured using COBAS MIRA system (Roche Diagnostics, Indianapolis, IN) by the Analytical Core of the Mouse Metabolic Phenotyping Center at Yale University (U24 DK059635).

Bile Acid Analysis

Liver extracts were analyzed by nano-electrospray ionization (ESI) mass spectrometry. The bile acid analyses were performed on a mass spectrometer PerkinElmer Sciex API-III (PerkinElmer, Alberta, Canada) modified with a nano-ESI source (Protana) as previously described (30).

Immunoblotting

Proteins in mouse liver lysates, Co-IP complex and primary mouse hepatocyte lysates were separated by SDS-PAGE and transferred to PVDF membranes. Primary antibodies (Supplemental Table 1) were incubated overnight at 4°C. Densitometric scanning of protein bands was performed using TotalLab TL100 software (TotalLab Ltd, Newcastle upon Tyne, UK).

Statistical Analysis

All data were subjected to outlier detection and analyzed using the nonparametric Kruskal-Wallis and Mann-Whitney tests offered in GraphPad Prism (GraphPad Software, La Jolla, CA). Values are expressed as the mean ± SD. A *P* value of less than 0.05 was considered significant.

RESULTS

1. Expression of NHERF-1 and ERM proteins as well as formation of ICAM-1-ERM-NHERF-1 complex are increased in mouse liver after bile duct ligation

To examine the roles of NHERF-1 and ERM proteins in neutrophil-mediated liver injury in cholestasis, we first examined the expression of NHERF-1 and ERM proteins in liver whole cell lysates of sham-operated and bile duct-ligated wild-type mice by immunoblotting. As shown in Fig. 2A, compared with the sham group, the expression levels of both NHERF-1 and total ERM proteins in BDL mouse liver were significantly increased ($P<0.05$). Since NHERF-1 is an ERM-binding protein and ERM proteins have been shown to interact with ICAM-1 and F-actin (21), we tested potential complex formation by these molecules in wild-type mouse liver. Co-immunoprecipitation was performed with liver lysates of sham-operated and bile duct-ligated mice using an anti-ICAM-1 antibody. We found that both NHERF-1 and ERM proteins were detected in the Co-IP complex along with ICAM-1 (Fig. 2B), confirming our hypothesis that ICAM-1, ERM proteins, NHERF-1 and F-actin form a macromolecule complex in mouse liver. We also observed that compared with the sham group, there was a dramatic increase in the abundance of ICAM-1, ERM proteins and NHERF-1 in the Co-IP complex from BDL mouse liver, suggesting that this complex plays a role in neutrophil-mediated liver injury after BDL.

2. NHERF-1$^{-/-}$ mice have reduced ERM and ICAM-1 protein expression in the liver and hepatocytes

To test whether NHERF-1 deficiency affects ERM protein expression in the liver, we next examined the expression levels of both total and phosphorylated ERM proteins in the liver of wild-type and NHERF-1$^{-/-}$ mice by immunoblotting. As shown in Fig. 3A, the expression of hepatic total ERM proteins in NHERF-1$^{-/-}$ sham mice was reduced to 52% of the WT mice ($P<0.05$) and the expression of phosphorylated ERM proteins in NHERF-1$^{-/-}$ mouse liver was further reduced to 38% of WT mice ($P<0.01$). After BDL, the phosphorylated ERM proteins remained reduced in NHERF-1$^{-/-}$ mouse liver, indicating that activated ERM proteins are reduced in the liver of NHERF-1$^{-/-}$BDL mice. Interestingly, the expression of hepatic total ERM proteins in NHERF-1$^{-/-}$ BDL mice was not significantly different from the WT mice, suggesting compensatory up-regulation of ERM proteins in NHERF-1$^{-/-}$ mouse liver after BDL.

Since ERM proteins have been shown to play a role in ICAM-1 expression in non-hepatic endothelial cells (23, 24), we then quantified the protein expression of ICAM-1 in both sham-operated and BDL mouse liver. As expected, ICAM-1 protein expression was significantly upregulated in both the WT and NHERF-1$^{-/-}$ mouse liver seven days after BDL (note that in Fig. 3B, compared with the sham samples, only half amount of total protein was loaded onto the gel for the BDL samples to avoid overloading). However, compared with the WT mice, hepatic ICAM-1 expression level was 40% lower in both sham-operated and BDL NHERF-1$^{-/-}$ mice ($P<0.01$; Fig. 3B). Using primary hepatocyte cultures, we also found that both ERM and ICAM-1 protein levels are dramatically reduced in NHERF-1$^{-/-}$ mouse hepatocytes compared with the WT mouse hepatocytes, and these proteins remain reduced after TNF-α stimulation (Fig. 3C), indicating that NHERF-1 has a

direct role in the expression of ERM proteins and ICAM-1 as well as the inflammatory response in hepatocytes. Further analysis of ICAM-1 mRNA expression by real-time PCR showed that compared with WT mice, hepatic ICAM-1 mRNA levels were not significantly different in NHERF-1$^{-/-}$ mice (Fig. 3D), suggesting that posttranscriptional regulation plays a primary role in the reduced expression of hepatic ICAM-1 protein in sham-operated and BDL NHERF-1$^{-/-}$ mice. Together these data demonstrated that NHERF-1 deficiency leads to reduction in the expression of ERM proteins and ICAM-1 in hepatocytes as well as sham and BDL mouse liver.

3. Neutrophil accumulation in the liver of NHERF-1$^{-/-}$ mice is significantly reduced after BDL

To examine whether disruption of the formation of ICAM-1-ERM-NHERF-1 complex as well as the decreased hepatic ERM protein and ICAM-1 expression in NHERF-1$^{-/-}$ mice results in reduced neutrophil infiltration in the liver, we assessed neutrophil accumulation in mouse liver by immunohistochemical staining. As shown in Fig. 4A, while sham-operated WT and NHERF-1$^{-/-}$ mice had very few neutrophil infiltrates in the liver parenchyma, a large number of neutrophils accumulated in and around the necrotic foci of hepatocytes in the liver of WT BDL mice. In contrast, only a limited number of neutrophils were detected in the liver of NHERF-1$^{-/-}$ BDL mice and very few infiltrated into the parenchyma. Statistical analysis with ImageJ on the stained liver sections revealed positive staining in 0.47±0.25% area in NHERF-1$^{-/-}$ BDL mice, a 47% reduction compared with the WT control that had 0.89±0.32% area of positive staining (P<0.05; Fig. 4B). Since β_2-integrins on neutrophils interact with ICAM-1 and participate in neutrophil infiltration as well, we also examined β_2-integrin expression on neutrophils from WT and NHERF-1$^{-/-}$ mice by flow cytometry. No significant difference was detected between the two groups (Supplemental Fig. S1), suggesting that it's unlikely that the reduced neutrophil infiltration in the liver of NHERF-1$^{-/-}$ BDL mice was due to a decrease in β_2-integrin expression on the neutrophils of these mice.

4. NHERF-1 $^{-/-}$ mice are protected from liver injury after BDL

As neutrophils play an important role in BDL induced liver injury, we then tested whether reduction of neutrophil infiltration in the livers of NHERF-1$^{-/-}$ mice results in reduced liver injury after BDL. As shown in Table 1, liver function analysis revealed that while serum levels of ALT in sham-operated WT and NHERF-1$^{-/-}$ mice were similar (24.7±5.6 U/L vs. 23.9±11.9 U/L), NHERF-1$^{-/-}$ BDL mice had 70% lower serum ALT activities compared with WT BDL mice (238.1±67.9 U/L vs. 890.0±325.9 U/L, P<0.001). In contrast, serum ALP levels were similar to WT BDL mice (780.0±391.6 U/L vs. 737.8±204.6 U/L), consistent with the finding of comparable levels of bile duct proliferation on histologic analysis (data not shown) even though NHERF-1$^{-/-}$ BDL mice had reduced levels of liver necrosis as noted in Fig. 5. No injury was detected in sham-operated WT and NHERF-1$^{-/-}$ mice. Seven days after BDL, the wild-type group had 13.2±5.0% area of necrotic foci. In contrast, the NHERF-1$^{-/-}$ BDL group had only 3.3±3.8% area of necrotic foci, which is 75% less than the WT BDL mice (P<0.05; Fig. 5A, 5B).

To test if the protective effects observed in NHERF-1$^{-/-}$ BDL mice were related to less cholestasis, we measured total bile acid levels in the serum and liver extracts. Surprisingly, total bile acid concentrations in either the serum or liver tissues of both sham and BDL NHERF-1$^{-/-}$ mice were not significantly different from the wild-type controls (Table 1), suggesting that the reduced liver injury in NHERF-1$^{-/-}$ BDL mice was not due to differences in bile acid concentrations in serum or liver. However, mass spectrometric analysis of hepatic bile acid composition revealed that while sham-operated WT and NHERF-1$^{-/-}$ mice had similar percentages of di- (9.47 ±2.54% vs. 10.71±2.45%), tri- (86.23±2.45% vs. 86.23±2.45%), and tetra-(4.3 ±0.95% vs. 2.78 ±1.27%) hydroxylated bile acids in the liver (P>0.05), compared to 8.53±2.62% in the WT BDL mice, the percentage of tetrahydroxylated bile acids increased to 14.3±0.74% in NHERF-1$^{-/-}$ BDL mouse liver (P<0.01; Fig. 6A). Real-time PCR also demonstrated that hepatic Cyp3a11 mRNA levels in NHERF-1$^{-/-}$ BDL mice were significantly increased compared with WT BDL mice (P<0.01; Fig. 6B), consistent with the change in bile acid profile and suggesting that upregulation of Cyp3a11 provided an additional mechanism in the adaptive response to cholestatic liver injury.

5. Induction of other pro-inflammatory genes in NHERF-1 $^{-/-}$ mice after BDL

Numerous studies indicate that other pro-inflammatory genes besides ICAM-1 are also upregulated in mouse liver and hepatocytes following bile duct ligation or bile acid treatment (11, 14). To determine if the expression levels of cytokines TNF-α and IL-1β, as well as chemokines Cxcl-2, Ccl-2 and Ccl-7 are also affected in NHERF-1$^{-/-}$ mice, the levels of their hepatic mRNA were assessed in sham-operated and BDL mice by real-time PCR. Our results showed that all these genes were greatly induced after BDL in livers of both WT and NHERF-1$^{-/-}$ mice. Additionally, sham-operated NHERF-1$^{-/-}$ mice had significantly higher levels of hepatic TNF-α, Cxcl-2, Ccl-2 and Ccl-7 mRNA levels than the WT control (P<0.05; Supplemental Fig. S2). However, NHERF-1$^{-/-}$ BDL mice showed a trend to lower Cxcl-2, Ccl-2 and Ccl-7 mRNA levels in the liver compared with WT BDL mice, although the reduction did not reach statistical significance (P>0.05; Supplemental Fig. S2).

DISCUSSION

In this study we tested the hypothesis that NHERF-1 assembles ERM proteins, ICAM-1 and F-actin into a macromolecule complex in mouse liver and deficiencies in NHERF-1 may affect expression of hepatic ERM proteins and ICAM-1, leading to reduced neutrophil accumulation and cholestatic liver injury induced by bile duct ligation. Our findings demonstrate that hepatic NHERF-1 and ERM proteins indeed co-immunoprecipitate with ICAM-1 and that formation of ICAM-1-ERM-NHERF-1 complex is increased after BDL. In addition, NHERF-1$^{-/-}$ mice have lower ERM and ICAM-1 protein expression in the liver and hepatocytes, in association with reduced hepatic neutrophil accumulation and attenuated liver injury after BDL. This attenuation in liver injury was also accompanied by an increase in the synthesis of tetrahydroxylated bile acid in the liver that was independent of total serum or hepatic bile acid concentrations.

As a versatile scaffolding protein that binds multiple partners and recruits functionally related proteins into integrated macromolecule complexes, NHERF-1 has been shown to participate in the expression, membrane localization and functional regulation of numerous membrane proteins such as cystic fibrosis transmembrane conductance regulator (CFTR) and β2-adrenergic receptor (32, 33). In mouse liver, NHERF-1 has been detected beneath the apical membrane of hepatocytes and cholangiocytes and has been shown to regulate the expression and function of multidrug resistance associated protein 2, an ATP-binding cassette transporter that plays an important role in bile formation and detoxification (25, 31). Similarly, ERM proteins also function as cross-linkers between cortical actin filaments and membrane proteins including ICAM-1. ICAM-1 plays a key role in adhesion and locomotion of adhered leukocytes to vascular endothelial cells during leukocyte extravasation across the endothelial barrier and their recruitment to the site of inflammation (20). In normal liver, ICAM-1 is barely detectable along the sinusoids and portal venules. In both BDL mice and patients with extrahepatic obstructive cholestasis, ICAM-1 is markedly upregulated in sinusoidal endothelial cells and is induced in hepatocytes in areas of parenchymal injury where the intensity of this induction correlates with the degree of liver damage (15, 34). Upon leukocyte-endothelium interaction, ICAM-1 becomes enriched in microvilli-like membrane projections and connects to the underlying F-actin through ERM proteins, forming a docking structure that anchors and partially embraces the leukocyte (21) (see Fig. 1). The interaction between ICAM-1 and activated ERM proteins is essential for leukocyte transendothelial migration (TEM) as deletion of a five amino acid segment in the intracellular domain of ICAM-1 abrogates its interaction with ERM proteins and significantly decreases leukocyte adhesion and subsequent TEM (35). Given the fact that increased formation of ICAM-1-ERM-NHERF-1 complex was detected in BDL mouse liver (Fig. 2) and that hepatocytes constitute about 80% of liver parenchymal cells, it is highly plausible that this macromolecule complex is formed in the cell cortex of sinusoidal endothelial cells as well as hepatocytes, and participates in neutrophil transendothelial and trans-hepatocyte migration after bile duct ligation. Deletion of NHERF-1 results in disruption of the formation of this complex as well as destabilization of ERM proteins and ICAM-1, leading to decreased cortical expression of these proteins, thereby reducing neutrophil transendothelial and trans-hepatocyte migration in the liver of NHERF-1$^{-/-}$ mice after BDL. On the other hand, deficiency in NHERF-1 might also attenuate the response of neutrophils to chemoattractants in BDL mice. Mañes et al showed that the interaction between NHERF-1/EBP50 and type I PIP5 kinase beta (PIP5KIβ) is necessary for PIP5KIβ localization and for chemoattractant-induced polarization of neutrophils (36). NHERF-1 assembles the CXC chemokine receptor CXCR2 and phospholipase C β_2 in neutrophils into a macromolecular signaling complex critical for neutrophil migration and infiltration (37). It is possible that NHERF-1 also affects the function of neutrophils in a similar manner during cholestatic liver injury.

The NF-κB transcription factor plays an essential role in the regulation of immune and inflammatory responses (38). Recently Leslie et al (39) showed that NHERF-1/EBP50 expression increased upon TNF-α treatment in primary macrophages and vascular smooth muscle cells and that this induction was NF-κB dependent. Conversely, deletion of NHERF-1 resulted in impaired activation of NF-κB in these cells. In NHERF-1$^{-/-}$ mice,

macrophage activation and recruitment to vascular lesions as well as vascular inflammation were reduced after LPS treatment. They also found that inflammatory stimuli promote the formation of an NHERF-1-PKCζ complex at the cell membrane that induces NF-κB signaling. They therefore concluded that NHERF-1 and NF-κB participate in a feed-forward loop leading to increased macrophage activation and enhanced response of vascular cells to inflammation. It remains to be determined whether this feed-forward loop also applies to the inflammatory response during BDL induced cholestasis. In the present study, we also observed that compared with sham mice, wild-type BDL mice have increased NHERF-1 expression in the liver (Fig. 2), accompanied by upregulation of total NF-κB p65 as well as phosphorylated NF-κB p65 (data not shown). In addition, expression of total NF-κB p65 as well as phosphorylated NF-κB p65 was significantly reduced in the liver of NHERF-$1^{-/-}$ BDL mice compared with WT BDL mice (data not shown). Activation of NF-κB has been detected in mouse hepatocytes and rat bile duct epithelium after BDL although it was reported that bile acids do not activate NF-κB in primary rat hepatocytes (40–42). However, the role of NF-κB in cholestatic liver injury remains controversial. Miyoshi et al reported that inhibition of NF-κB activation potentiated hepatocyte apoptosis and liver injury in BDL mice and concluded that activated NF-κB functions to reduce liver injury (40). In contrast, Demirbilek et al showed that NF-κB inhibitors attenuated liver injury in BDL rats (41). Future studies on the function of NF-κB in the inflammatory response as well as the relationship between NHERF-1 and NF-κB in BDL mice would be of interest in further understanding of roles of NHERF-1 and NF-κB in cholestatic liver injury.

In summary, our study demonstrates that NHERF-1 assembles ERM proteins, ICAM-1 and F-actin into a macromolecule complex in mouse liver and deletion of NHERF-1 in mice leads to a reduced expression of hepatic ERM proteins and ICAM-1, molecules that are up-regulated and are essential for neutrophil migration and infiltration after bile duct ligation. NHERF-1 deficiency also increased synthesis of tetrahydroxylated bile acid in the liver after BDL. These multiple mechanisms protect NHERF-$1^{-/-}$ mice against cholestatic liver injury induced by bile duct ligation. Further study of the role of NHERF-1 in the inflammatory response in cholestatic and other forms of liver injury should lead to discovery of new therapeutic targets in cholestasis and other hepatic inflammatory diseases.

Supplementary Material

Refer to Web version on PubMed Central for supplementary material.

ACKNOWLEDGEMENT

We thank Kathy Harry for excellent technical assistance.

Financial Support

This work was supported by National Institutes of Health National Institute of Diabetes and Digestive and Kidney Diseases grants DK R37 25636 and DK P30-34989.

List of Abbreviations

ICAM-1	intercellular adhesion molecule-1
BDL	bile duct ligation
ERM	ezrin-radixin-moesin
NHERF-1	Na+/H+ exchanger regulatory factor 1
EBP50	ERM-binding phosphoprotein 50
TNF-α	tumor necrosis factor α
VCAM-1	vascular cell adhesion molecule-1
HUVEC	human umbilical vein endothelial cells
PIP2	phosphatidylinositol 4, 5-bisphosphate
ALT	aminotransferase
ALP	alkaline phosphatase
CFTR	cystic fibrosis transmembrane conductance regulator
TEM	transendothelial migration
PIP5Kiβ	type I PIP5 kinase beta
FACS	fluorescence-activated cell sorting

Reference List

1. Hirschfield GM, Heathcote EJ, Gershwin ME. Pathogenesis of cholestatic liver disease and therapeutic approaches. Gastroenterology. 2010 Nov; 139(5):1481–1496. [PubMed: 20849855]
2. Penz-Osterreicher M, Osterreicher CH, Trauner M. Fibrosis in autoimmune and cholestatic liver disease. Best Pract Res Clin Gastroenterol. 2011 Apr; 25(2):245–258. [PubMed: 21497742]
3. Higuchi H, Gores GJ. Bile acid regulation of hepatic physiology: IV. Bile acids and death receptors. Am J Physiol Gastrointest Liver Physiol. 2003 May; 284(5):G734–G738. [PubMed: 12684208]
4. Perez MJ, Briz O. Bile-acid-induced cell injury and protection. World J Gastroenterol. 2009 Apr 14; 15(14):1677–1689. [PubMed: 19360911]
5. Maillette de Buy WL, Beuers U. Bile salts and cholestasis. Dig Liver Dis. 2010 Jun; 42(6):409–418. [PubMed: 20434968]
6. Benz C, Angermuller S, Kloters-Plachky P, Sauer P, Stremmel W, Stiehl A. Effect of S-adenosylmethionine versus tauroursodeoxycholic acid on bile acid-induced apoptosis and cytolysis in rat hepatocytes. Eur J Clin Invest. 1998 Jul; 28(7):577–583. [PubMed: 9726039]
7. Faubion WA, Guicciardi ME, Miyoshi H, Bronk SF, Roberts PJ, Svingen PA, et al. Toxic bile salts induce rodent hepatocyte apoptosis via direct activation of Fas. J Clin Invest. 1999 Jan; 103(1):137–145. [PubMed: 9884343]
8. Reinehr R, Graf D, Haussinger D. Bile salt-induced hepatocyte apoptosis involves epidermal growth factor receptor-dependent CD95 tyrosine phosphorylation. Gastroenterology. 2003 Sep; 125(3): 839–853. [PubMed: 12949729]
9. Schoemaker MH, Conde dlR, Buist-Homan M, Vrenken TE, Havinga R, Poelstra K, et al. Tauroursodeoxycholic acid protects rat hepatocytes from bile acid-induced apoptosis via activation of survival pathways. Hepatology. 2004 Jun; 39(6):1563–1573. [PubMed: 15185297]

10. Woolbright BL, Li F, Xie Y, Farhood A, Fickert P, Trauner M, et al. Lithocholic acid feeding results in direct hepato-toxicity independent of neutrophil function in mice. Toxicol Lett. 2014 Jul 3; 228(1):56–66. [PubMed: 24742700]
11. Allen K, Jaeschke H, Copple BL. Bile acids induce inflammatory genes in hepatocytes: a novel mechanism of inflammation during obstructive cholestasis. Am J Pathol. 2011 Jan; 178(1):175–186. [PubMed: 21224055]
12. Woolbright BL, Jaeschke H. Novel insight into mechanisms of cholestatic liver injury. World J Gastroenterol. 2012 Sep 28; 18(36):4985–4993. [PubMed: 23049206]
13. Georgiev P, Jochum W, Heinrich S, Jang JH, Nocito A, Dahm F, et al. Characterization of time-related changes after experimental bile duct ligation. Br J Surg. 2008 May; 95(5):646–656. [PubMed: 18196571]
14. Zhang Y, Hong JY, Rockwell CE, Copple BL, Jaeschke H, Klaassen CD. Effect of bile duct ligation on bile acid composition in mouse serum and liver. Liver Int. 2012 Jan; 32(1):58–69. [PubMed: 22098667]
15. Gujral JS, Liu J, Farhood A, Hinson JA, Jaeschke H. Functional importance of ICAM-1 in the mechanism of neutrophil-induced liver injury in bile duct-ligated mice. Am J Physiol Gastrointest Liver Physiol. 2004 Mar; 286(3):G499–G507. [PubMed: 14563671]
16. Lawson C, Wolf S. ICAM-1 signaling in endothelial cells. Pharmacol Rep. 2009 Jan; 61(1):22–32. [PubMed: 19307690]
17. Ramaiah SK, Jaeschke H. Role of neutrophils in the pathogenesis of acute inflammatory liver injury. Toxicol Pathol. 2007 Oct; 35(6):757–766. [PubMed: 17943649]
18. Fehon RG, McClatchey AI, Bretscher A. Organizing the cell cortex: the role of ERM proteins. Nat Rev Mol Cell Biol. 2010 Apr; 11(4):276–287. [PubMed: 20308985]
19. Wittchen ES. Endothelial signaling in paracellular and transcellular leukocyte transmigration. Front Biosci (Landmark Ed). 2009; 14:2522–2545. [PubMed: 19273217]
20. Reglero-Real N, Marcos-Ramiro B, Millan J. Endothelial membrane reorganization during leukocyte extravasation. Cell Mol Life Sci. 2012 Sep; 69(18):3079–3099. [PubMed: 22573182]
21. Barreiro O, Yanez-Mo M, Serrador JM, Montoya MC, Vicente-Manzanares M, Tejedor R, et al. Dynamic interaction of VCAM-1 and ICAM-1 with moesin and ezrin in a novel endothelial docking structure for adherent leukocytes. J Cell Biol. 2002 Jun 24; 157(7):1233–1245. [PubMed: 12082081]
22. Carman CV, Jun CD, Salas A, Springer TA. Endothelial cells proactively form microvilli-like membrane projections upon intercellular adhesion molecule 1 engagement of leukocyte LFA-1. J Immunol. 2003 Dec 1; 171(11):6135–6144. [PubMed: 14634129]
23. Aranda JF, Reglero-Real N, Marcos-Ramiro B, Ruiz-Saenz A, Fernandez-Martin L, Bernabe-Rubio M, et al. MYADM controls endothelial barrier function through ERM-dependent regulation of ICAM-1 expression. Mol Biol Cell. 2013 Feb; 24(4):483–494. [PubMed: 23264465]
24. Koss M, Pfeiffer GR, Wang Y, Thomas ST, Yerukhimovich M, Gaarde WA, et al. Ezrin/radixin/moesin proteins are phosphorylated by TNF-alpha and modulate permeability increases in human pulmonary microvascular endothelial cells. J Immunol. 2006 Jan 15; 176(2):1218–1227. [PubMed: 16394012]
25. Fouassier L, Duan CY, Feranchak AP, Yun CH, Sutherland E, Simon F, et al. Ezrin-radixin-moesin-binding phosphoprotein 50 is expressed at the apical membrane of rat liver epithelia. Hepatology. 2001 Jan; 33(1):166–176. [PubMed: 11124833]
26. Minkoff C, Shenolikar S, Weinman EJ. Assembly of signaling complexes by the sodium-hydrogen exchanger regulatory factor family of PDZ-containing proteins. Curr Opin Nephrol Hypertens. 1999 Sep; 8(5):603–608. [PubMed: 10541224]
27. Morales FC, Takahashi Y, Kreimann EL, Georgescu MM. Ezrin-radixin-moesin (ERM)-binding phosphoprotein 50 organizes ERM proteins at the apical membrane of polarized epithelia. Proc Natl Acad Sci U S A. 2004 Dec 21; 101(51):17705–17710. [PubMed: 15591354]
28. Shenolikar S, Voltz JW, Minkoff CM, Wade JB, Weinman EJ. Targeted disruption of the mouse NHERF-1 gene promotes internalization of proximal tubule sodium-phosphate cotransporter type IIa and renal phosphate wasting. Proc Natl Acad Sci U S A. 2002 Aug 20; 99(17):11470–11475. [PubMed: 12169661]

29. Gartung C, Ananthanarayanan M, Rahman MA, Schuele S, Nundy S, Soroka CJ, et al. Down-regulation of expression and function of the rat liver Na+/bile acid cotransporter in extrahepatic cholestasis. Gastroenterology. 1996 Jan; 110(1):199–209. [PubMed: 8536857]
30. Soroka CJ, Mennone A, Hagey LR, Ballatori N, Boyer JL. Mouse organic solute transporter alpha deficiency enhances renal excretion of bile acids and attenuates cholestasis. Hepatology. 2010 Jan; 51(1):181–190. [PubMed: 19902485]
31. Li M, Wang W, Soroka CJ, Mennone A, Harry K, Weinman EJ, et al. NHERF-1 binds to Mrp2 and regulates hepatic Mrp2 expression and function. J Biol Chem. 2010 Jun 18; 285(25):19299–19307. [PubMed: 20404332]
32. Swiatecka-Urban A, Duhaime M, Coutermarsh B, Karlson KH, Collawn J, Milewski M, et al. PDZ domain interaction controls the endocytic recycling of the cystic fibrosis transmembrane conductance regulator. J Biol Chem. 2002 Oct 18; 277(42):40099–40105. [PubMed: 12167629]
33. Cao TT, Deacon HW, Reczek D, Bretscher A, von ZM. A kinase-regulated PDZ-domain interaction controls endocytic sorting of the beta2-adrenergic receptor. Nature. 1999 Sep 16; 401(6750):286–290. [PubMed: 10499588]
34. Gulubova MV. Intercellular adhesion molecule-1 (ICAM-1) expression in the liver of patients with extrahepatic cholestasis. Acta Histochem. 1998 Feb; 100(1):59–74. [PubMed: 9542581]
35. Oh HM, Lee S, Na BR, Wee H, Kim SH, Choi SC, et al. RKIKK motif in the intracellular domain is critical for spatial and dynamic organization of ICAM-1: functional implication for the leukocyte adhesion and transmigration. Mol Biol Cell. 2007 Jun; 18(6):2322–2335. [PubMed: 17429072]
36. Manes S, Fuentes G, Peregil RM, Rojas AM, Lacalle RA. An isoform-specific PDZ-binding motif targets type I PIP5 kinase beta to the uropod and controls polarization of neutrophil-like HL60 cells. FASEB J. 2010 Sep; 24(9):3381–3392. [PubMed: 20442317]
37. Wu Y, Wang S, Farooq SM, Castelvetere MP, Hou Y, Gao JL, et al. A chemokine receptor CXCR2 macromolecular complex regulates neutrophil functions in inflammatory diseases. J Biol Chem. 2012 Feb 17; 287(8):5744–5755. [PubMed: 22203670]
38. Luedde T, Schwabe RF. NF-kappaB in the liver--linking injury, fibrosis and hepatocellular carcinoma. Nat Rev Gastroenterol Hepatol. 2011 Feb; 8(2):108–118. [PubMed: 21293511]
39. Leslie KL, Song GJ, Barrick S, Wehbi VL, Vilardaga JP, Bauer PM, et al. Ezrin-radixin-moesin-binding phosphoprotein 50 (EBP50) and nuclear factor-kappaB (NF-kappaB): a feed-forward loop for systemic and vascular inflammation. J Biol Chem. 2013 Dec 20; 288(51):36426–36436. [PubMed: 24196963]
40. Miyoshi H, Rust C, Guicciardi ME, Gores GJ. NF-kappaB is activated in cholestasis and functions to reduce liver injury. Am J Pathol. 2001 Mar; 158(3):967–975. [PubMed: 11238044]
41. Demirbilek S, Akin M, Gurunluoglu K, Aydin NE, Emre MH, Tas E, et al. The NF-kappaB inhibitors attenuate hepatic injury in bile duct ligated rats. Pediatr Surg Int. 2006 Aug; 22(8):655–663. [PubMed: 16830161]
42. Schoemaker MH, Gommans WM, Conde dlR, Homan M, Klok P, Trautwein C, et al. Resistance of rat hepatocytes against bile acid-induced apoptosis in cholestatic liver injury is due to nuclear factor-kappa B activation. J Hepatol. 2003 Aug; 39(2):153–161. [PubMed: 12873810]
43. Boyer JL, Phillips JM, Graf J. Preparation and specific applications of isolated hepatocyte couplets. Methods Enzymol. 1990; 192:501–516. [PubMed: 1963665]

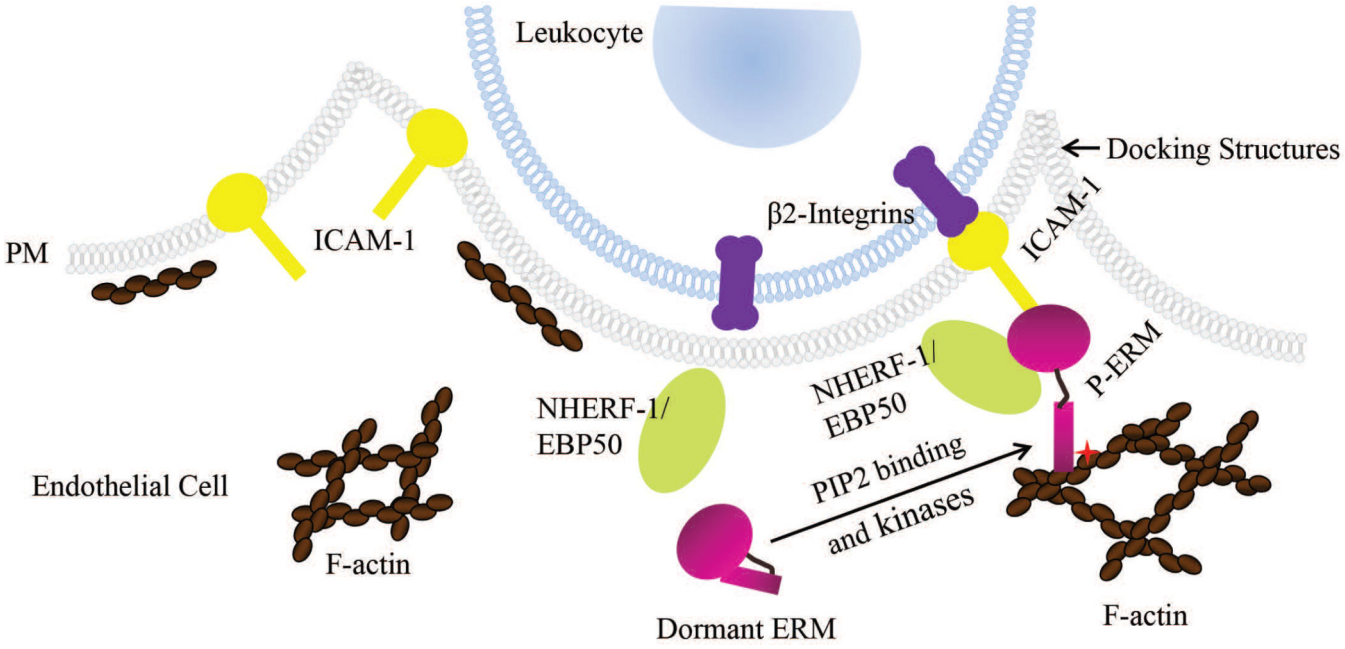

Fig. 1.

ICAM-1 and ERM proteins participate in leukocyte transendothelial migration. ICAM-1 is localized at the apical membrane of endothelial cells and is upregulated under inflammatory conditions. Upon leukocyte-endothelium interaction, ICAM-1 interacts with β2-integrins that are expressed on the cell surface of leukocytes and is connected to the underlying F-actin network through scaffolding proteins such as activated ERM proteins in microvilli-like membrane projections. These “docking” structures anchor and partially embrace the leukocyte to promote firm leukocyte adhesion and initiate leukocyte transendothelial migration. NHERF-1/EBP50, a PDZ protein, interacts with ERM proteins. We propose in the current study that NHERF-1 assembles ERM proteins, ICAM-1 and F-actin into a macromolecule complex in the cell cortex of sinusoidal endothelial cells as well as hepatocytes in mouse liver and that this complex participates in neutrophil transendothelial and trans-hepatocyte migration after bile duct ligation.

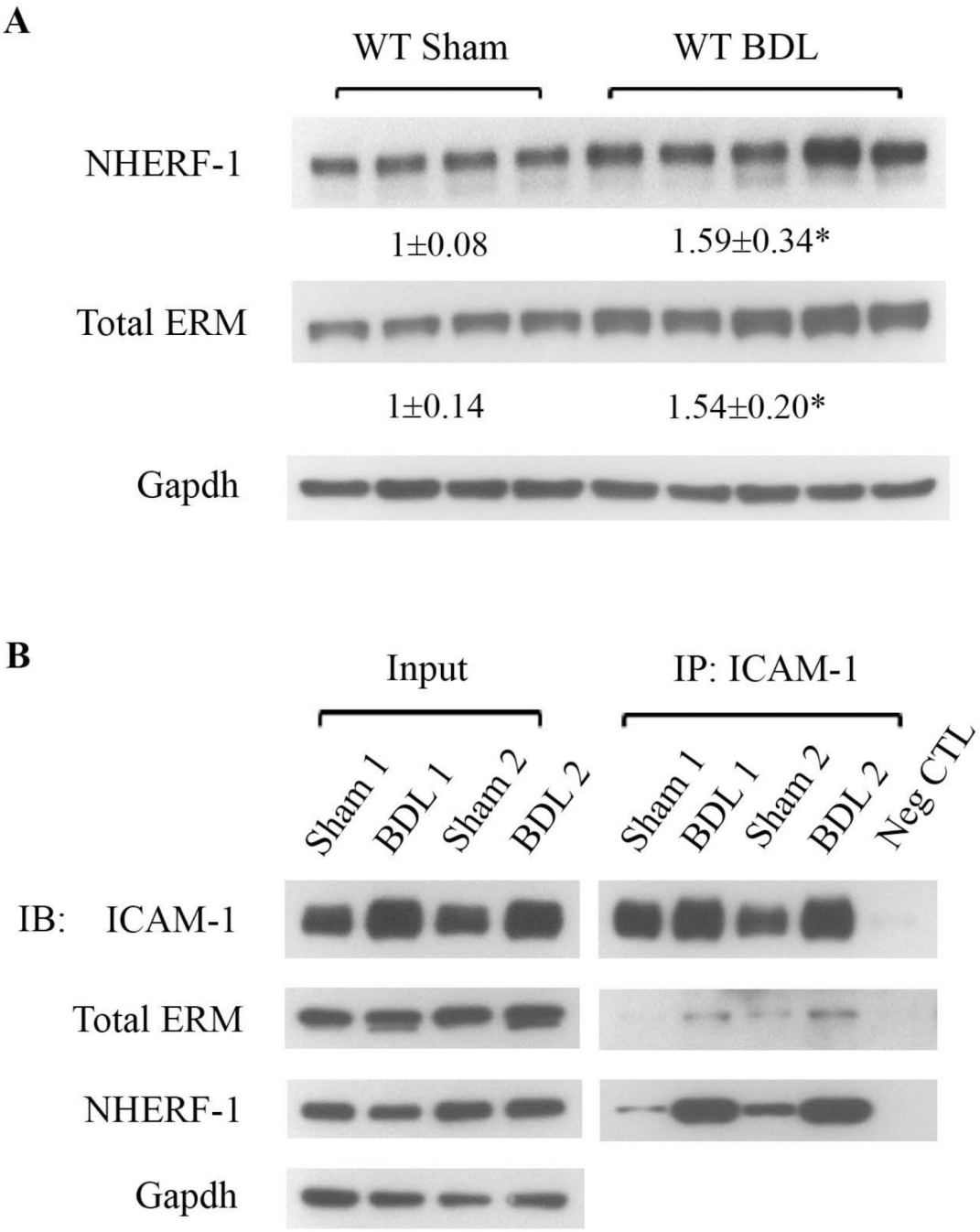

Fig. 2.

Expression of NHERF-1 and ERM proteins as well as formation of ICAM-1-ERM-NHERF-1 complex are increased in mouse liver after bile duct ligation. **A**. Representative immunoblots of whole cell lysates from wild-type mouse liver tissue showing significant increase in the levels of NHERF-1 and total ERM proteins in wild-type BDL mice compared with sham-operated mice. The relative ratio of the respective protein bands in sham and BDL mice was determined by densitometric analysis and normalized to Gapdh. The amount of protein from the sham group is set as 1. Values represent the means ± SD of 4 or 5

animals in each group. *P<0.05. **B.** Representative immunoblots of co-immunoprecipitation (Co-IP). Liver lysates of sham-operated or BDL wild-type mice were immunoprecipated with an anti-ICAM-1 antibody. In each Co-IP reaction, 10 μg of the antibody was immobilized to 25 μl of the agarose resin and incubated with 4 mg pre-cleared liver protein. The lysates (Input) and the immunoprecipitate (IP) complex were immunoblotted with anti-ICAM-1, anti-total ERM, anti-NHERF-1 or anti-Gapdh as indicated. n=4 in the sham or BDL group. Note the dramatic increase in the abundance of ICAM-1, ERM proteins and NHERF-1 in the Co-IP complex from BDL liver lysates compared with the sham liver lysates. Neg CTL: negative control. IB: immunoblotting.

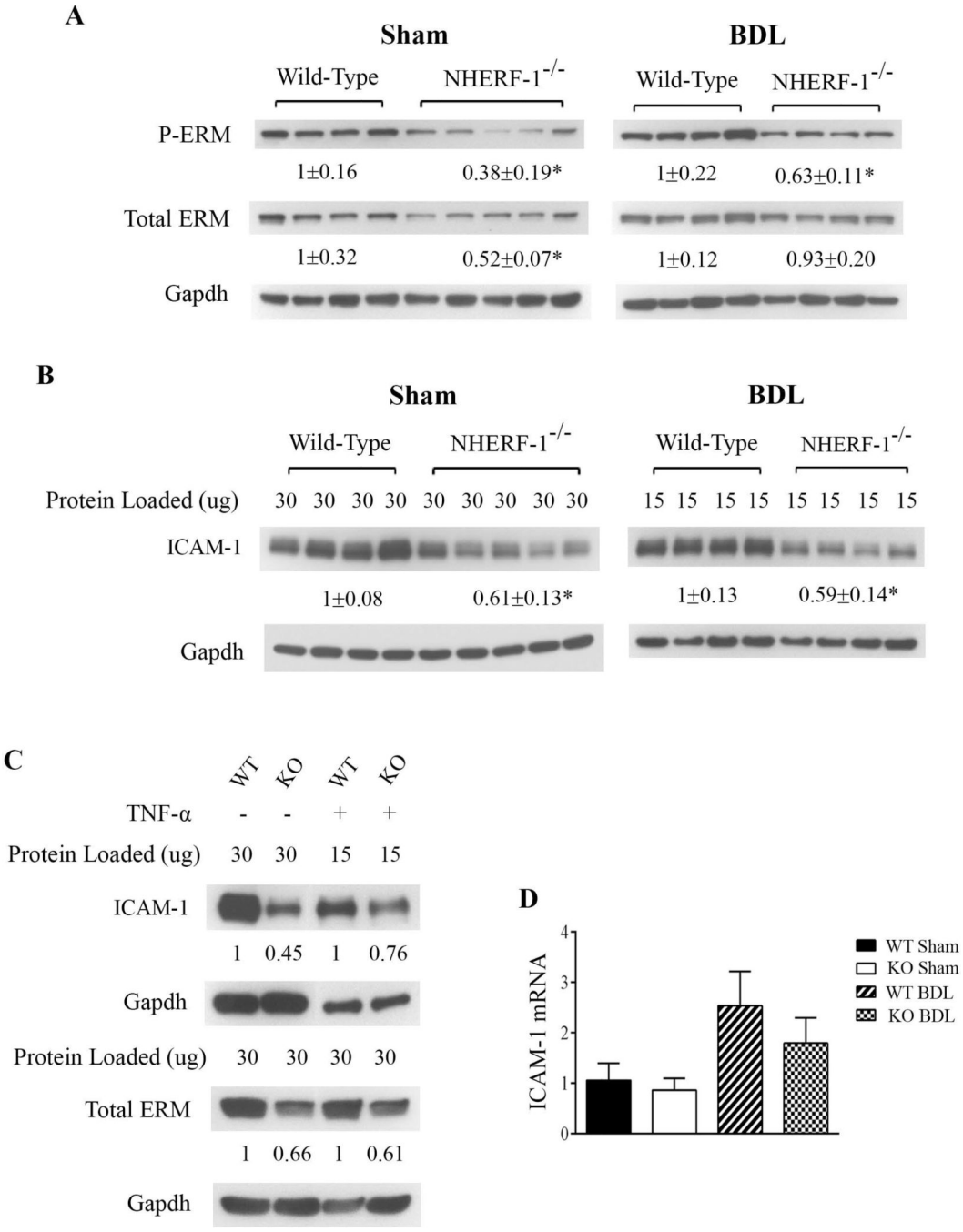

Fig. 3.

NHERF-1$^{-/-}$ mice have significantly reduced ERM and ICAM-1 protein expression in the liver and hepatocytes. Representative immunoblots of whole cell lysates from mouse liver tissue (**A** and **B**) and primary mouse hepatocytes (**C**) demonstrating significant reduction in total ERM, phosphorylated ERM and ICAM-1 proteins in NHERF-1$^{-/-}$ sham and BDL mice compared with wild-type sham and BDL mice. In **A, B** and **C**, the relative ratio of the respective protein bands in wild-type and NHERF-1$^{-/-}$ mice was determined by densitometric analysis and normalized to Gapdh. The amount of protein from the wild-type

is set as 1. In **A** and **B**, values represent the means ± SD of 4 or 5 animals in each group. In **B**, 30 μg of protein from each of the sham samples was loaded onto the gel whereas only 15 μg of protein from each of the BDL samples was loaded in order to avoid overloading. In **C**, primary hepatocytes were isolated from wild-type and NHERF-1$^{-/-}$ mice and cultured as described in Supplemental Materials. Whole cell lysates of untreated primary hepatocytes or primary hepatocytes treated with TNF-α (10 ng/ml) for 6 hr were subjected to immunoblotting. n=2 in each group. **D**. Relative levels of ICAM-1 mRNA in the liver of wild-type and NHERF-1$^{-/-}$ mice quantified by real-time PCR. Data are normalized to Gapdh, and the amount of hepatic ICAM-1 mRNA from wild-type sham mice is set as 1. Values represent the means ± SD of 6–9 individual animals in each group. WT: wild-type. KO: NHERF-1$^{-/-}$. *P<0.05.

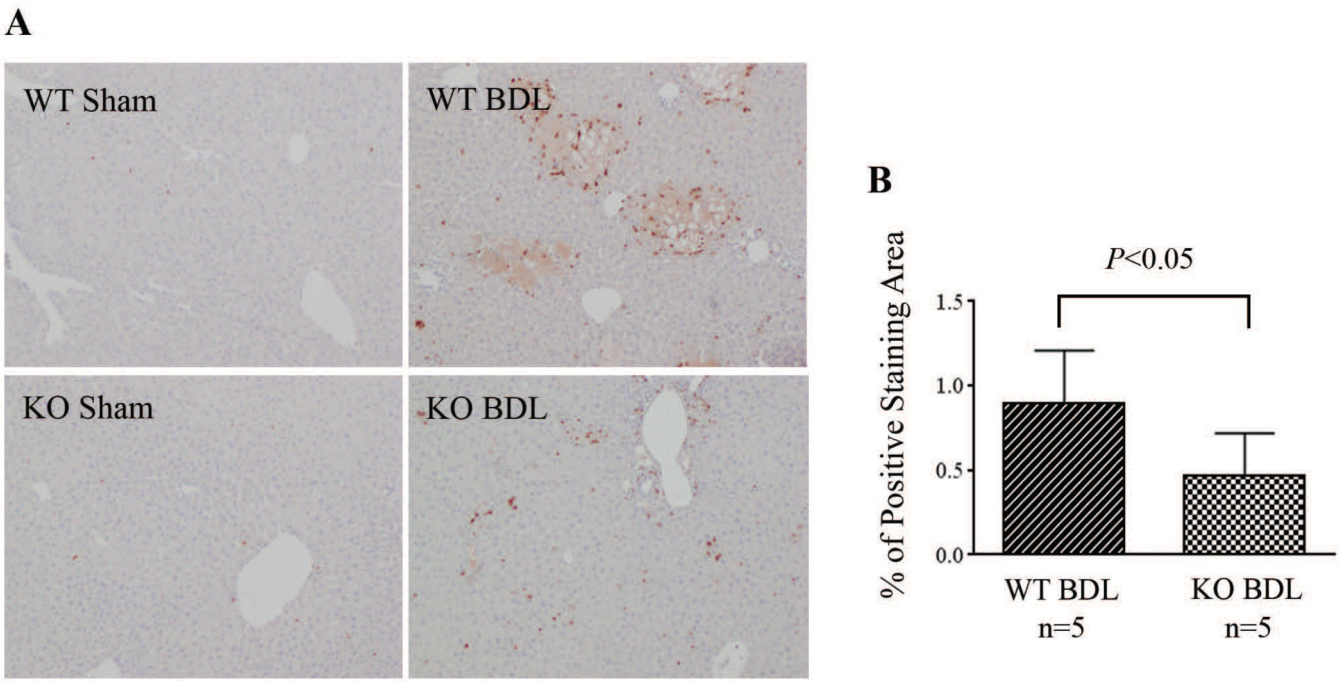

Fig. 4.

Neutrophil accumulation in the liver is significantly reduced in NHERF-1$^{-/-}$ BDL mice. **A**. Immunohistochemical staining of neutrophils on liver sections. Note that a large number of neutrophils accumulated in the liver in wild-type BDL mice, mostly detected in and around the necrotic foci of hepatocytes. In contrast, only a limited number of neutrophils were detected in the liver parenchyma of NHERF-1$^{-/-}$ BDL mice. **B**. Morphometry of neutrophil accumulation in BDL mouse liver by ImageJ. Data represents means ± SD of percentage of positive staining area on 10 random images (10x magnification) per animal from 5 animals in each group. WT: wild-type. KO: NHERF-1$^{-/-}$.

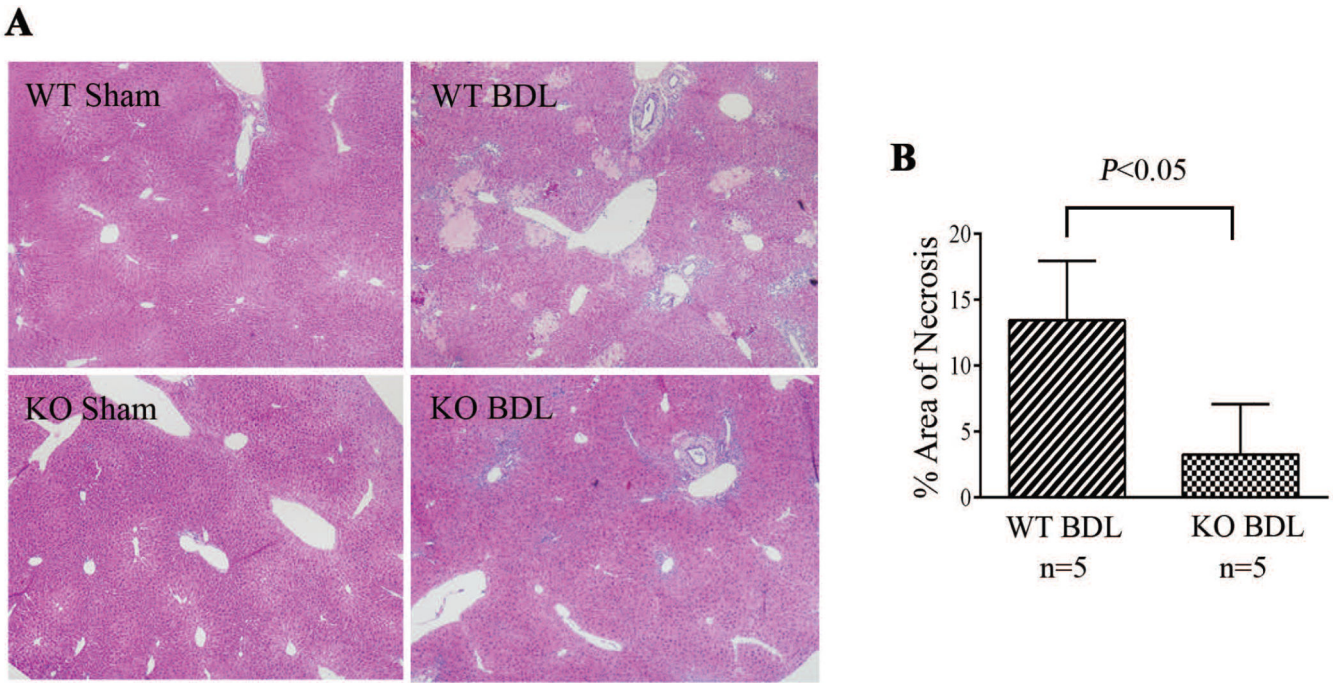

Fig. 5.

Liver necrosis was significantly lower in NHERF-1$^{-/-}$ BDL mice compared with wild-type BDL mice. **A.** H&E staining of liver sections of sham operated and BDL mice. **B.** Morphometry of liver necrosis in BDL mice. Data represents means ± SD of 5 animals in each group. Note that no necrosis was detected in both wild-type and NHERF-1$^{-/-}$ sham mouse liver. However, the wild-type BDL group had 14% area of liver necrosis foci, whereas the NHERF-1$^{-/-}$ BDL group had only 3% area of liver necrosis foci. WT: wild-type. KO: NHERF-1$^{-/-}$.

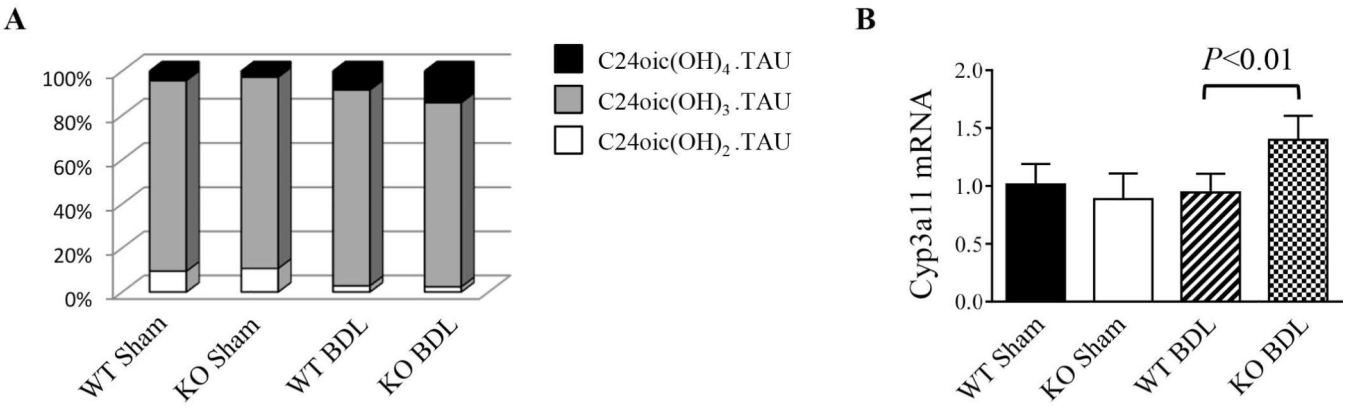

Fig. 6.

A. Analysis of hepatic bile acid composition by mass spectrometry. Dihydroxylated, trihydroxylated and tetrahydroxylated bile acids from liver extract was quantified and normalized to the total detectable bile acids for each animal. Note that WT and NHERF-1$^{-/-}$ sham mice had similar percentages of dihydroxylated, trihydroxylated and tetrahydroxylated bile acids. After BDL, the percentage of tetrahydroxylated bile acids increased to 14.3±0.74% in NHERF-1$^{-/-}$ mice, which is significantly higher than the 8.53±2.62% in WT BDL mice (P<0.01). n=5 or 6 in each group. **B.** Quantification of hepatic Cyp3a11 mRNA levels by real-time PCR. Data are normalized to Gapdh, and the amount of hepatic Cyp3a11 mRNA from wild-type sham mice is set as 1. Values represent the means ± SD of 5 or 6 animals in each group. WT: wild-type. KO: NHERF-1$^{-/-}$.

Table 1

Serum parameters and liver bile acid concentration of wild-type and NHERF-1$^{-/-}$ mice

Parameter	WT Sham	NHERF-1$^{-/-}$ Sham	WT BDL	NHERF-1$^{-/-}$ BDL
Serum ALT (U/L)	24.7±5.6	23.9±11.9	890.0±325.9	238.1±67.9***
Serum ALP (U/L)	73.7±8.5	72.2±10.2	737.8±204.6	780.0±391.6
Serum bile acids (μM)	8.15±7.3	30.7±31.4	278.3±75.3	303.4±78.0
Liver bile acids (nmol/g liver)	136.5±46.0	152.1±58.6	402.1±127.2	347.5±63.8

Data represent mean ± SD of n = 5–10. ALT, aminotransferase;ALP, alkaline phosphatase;

*** P<0.001, NHERF-1$^{-/-}$ BDL mice vs. WT BDL mice.